Noninvasive Blood Pressure and the Second Heart Sound Analysis

Ana Castro[1], Sandra S. Mattos[2] and Miguel T. Coimbra[3]

Abstract— **Heart sound characteristics are linked to blood pressure, and its interpretation is important for detection of cardiovascular disease. In this study, heart sounds' auscultation, acquired from children patients (27 patients, 10.2±3.9 years, 35.7±20.8 kg, 132.3±25.5 cm), were automatically segmented to extract the two main components: the first sound (S1) and the second sound (S2). Following, a set of time, frequency, and wavelet based features, were extracted from the S2, and analyzed in relation to the noninvasive cuff-based measures of blood pressure (mean blood pressure of 78±8.8 mmHg). A multivariate regression analysis was performed for each S2 feature set to determine which features better related to the blood pressure measurements. The best results, in the leave-one-out evaluation, were obtained using the frequency features set, with a MAE of 6.08 mmHg, a MAPE of 7.85%, and a ME of 0.31 mmHg, in the estimation of the mean blood pressure.**

I. INTRODUCTION

Home health monitoring is gaining greater interest for distinct reasons, such as safety, comfort, and costs reduction. This reality demands for simpler and wearable health monitors, that allow for a continuous record of physiological signals, as little invasive as possible, and without discomfort for the patient [1]. The World Health Organization estimates that high blood pressure (BP) or hypertension (HT) is the cause of 7.5 million deaths each year, corresponding to 12.8% of deaths. HT is also a risk factor for strokes, heart attacks and heart failure, renal impairment, peripheral vascular disease and retinopathy [2].

Home health monitoring systems may bring benefits from the perspective of both patients, physicians, and health care providers. From the patient's side, these systems allow a myriad of opportunities, from remotely monitoring chronic patients, to promoting wellness and self-care to others, improving their outcomes. From the physicians and health care providers' side these technologies help to cut direct health care costs by reducing the number of hospitalizations, also reducing the risks of hospital-acquired infections, and hospitalization overcrowding. Moreover, these technologies may help to extend the health care to patients who live in places far from a medical center.

[1]A. Castro is with Faculdade de Engenharia, Universidade do Porto, Portugal ana.castro@dcc.fc.up.pt

[2]S. S. Mattos is with Unidade de Cardiologia e Medicina Fetal, Real Hospital Português, Recife, Brasil ssmattos@cardiol.br

[3]M. T. Coimbra is with Instituto de Telecomunicações, Faculdade de Ciências, Departamento de Ciência de Computadores, Universidade do Porto, Portugal mcoimbra@dcc.fc.up.pt

This work was partially funded by the Fundação para a Ciência e Tecnologia (FCT, Portuguese Foundation for Science and Technology) under the reference Heart Safe PTDC/EEI-PRO/2857/2012; and Project I-CITY - ICT for Future Health/Faculdade de Engenharia da Universidade do Porto, NORTE-07-0124-FEDER-000068.

Usually BP is measured by cuff-based noninvasive methods, or through an arterial catheter placed in the radial artery with a pressure transducer (invasive). These methods are uncomfortable and inadequate for long term monitoring, and several techniques to substitute the current standard are being explored for the continuous noninvasive BP estimation, with as little apparatus as possible, applying different physiological properties of the cardiovascular system, such as the Pulse Transit Time (PTT) [1], vascular transit time (VTT) [3], and the heart sound [4], [5], [6]. Since increased BP leads to an increase in amplitude and frequency of the second heart sound [7], we propose to explore heart sound as a noninvasive BP correlate.

A heart cycle period (S11) is depicted in four main components [8]: the first sound (S1), the systolic period (S12), the second sound (S2), and the diastolic period (S21), as illustrated in the phonocardiogram (PCG) in Figure 1. The correct identification of heart sounds allows retrieval of information from each component, including the detection of murmurs and its characteristics.

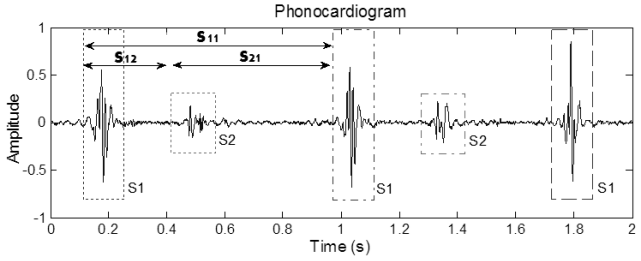

Fig. 1: Phonocardiogram (PCG) representation, with correspondent heart sound components: first sound (S_1), second sound (S_2), systolic (S_{12}), diastolic (S_{21}) and heart cycle (S_{11}) periods.

The S2 is described as being composed by two components: the first related to the closure of the aortic valve (A2) and systemic BP, and a second component related to the closure of the pulmonary valve (P2) and pulmonary BP [8], [6]. Previous studies have demonstrated a relation between S2 and the arterial pressure both on the systemic [4] and pulmonary circulations [6], [5].

In this study, time-frequency features extracted from the S2 were analyzed in relation to the noninvasive peripheral BP measures.

II. MATERIAL AND METHODS

Data collected in the Real Hospital Português (RHP) in Recife, Brasil, with a Littmann® 3200 electronic stethoscope

TABLE I: Sample mean, standard-deviation, and range values of the demographic data, and blood pressure measurements.

	Age (years)	Weight (kg)	Height (cm)	SBP (mmHg)	DBP (mmHg)	MBP (mmHg)
Mean	10.2	35.7	132.3	104.6	64.7	78.0
Standard-Deviation	3.9	20.8	25.5	12.9	8.4	8.8
Range (min-max)	3-18	8-97	69-183	90-145	50-90	63.3-103.3

(4 kHz), and the DigiScope Collector (Figure 2). Data were anonymized and shipped to Portugal with the approval of the RHP and University of Porto Ethics Commitees. Noninvasive systemic BP was measured in the arm and sitting position. Collected demographic data include gender, age, weight and height. Data analysis performed in MATLAB R2013b.

Fig. 2: DigiScope Collector system prototype front view.

A. Data Set

Data collected from 27 patients, 10 female. Table I presents the sample demographic data and BP values.

To analyze the relation between S2 characteristics and the individual BP, Mean Blood Pressure (MBP) was approximated using systolic and diastolic BP (SBP, DBP) measurements, according to Equation 1 [9].

$$MBP \approx \frac{2DBP + SBP}{3} \tag{1}$$

B. Heart Sound Segmentation

Heart sound segmentation was performed on PCGs collected over the pulmonary auscultation spot, as described in [10]. Figure 3 presents an example of the segmentation results.

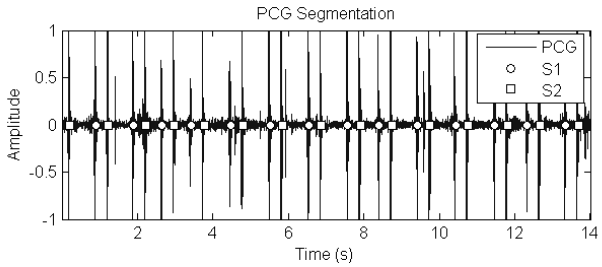

Fig. 3: Segmentation of a phonocardiogram with corresponding detected S1 (circle) and S2 (square) marks.

Total auscultation time in the pulmonary spot was of 307.5 s (432 detected S2s).

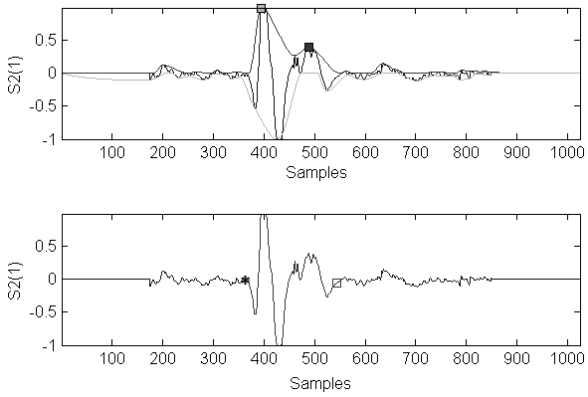

Fig. 4: On top, example of the temporal positive and negative contour envelopes; on bottom, representation of a S2 and corresponding detected delimiters.

C. Heart Sound Features Extraction

Following heart sound segmentation, detected S2s were analyzed for each patient, and time and frequency based features extracted as described below.

Temporal contour envelopes were extracted from each S2, based on the local maximums and minimums of the signal, and interpolated using a cubic Hermitian spline (Figure 4). For each positive envelope, the two largest peaks are detected: the first corresponding to the A2 component, and the second to an estimated P2 (difficult S2 segmentation validation). The lag between peaks was also extracted.

Similarly, the energy of the signal was obtained (Equation 2), and the peaks of the energy envelope extracted as before (A2, P2, and lag).

$$E = \frac{1}{win} \sum_{i=1}^{win} PCG(i)^2 \tag{2}$$

where win is the window length.

To extract information regarding solely activity during an S2, an algorithm based on the difference between positive and negative contour envelopes was developed to extract the signal periods of sound and silence (10% threshold). The developed algorithm brings additional information regarding S2 duration, which was also stored. Figure 4 presents an example of a S2 delimitation. For each delimited S2 the zero-crossing rate of the segment was obtained.

Shannon entropy was also extracted from each S2 (Equation 3) [11].

$$Entropy = \frac{1}{n} \sum_{i=1}^{n} p_i log(p_i) \tag{3}$$

for a set of events with PDF $\{p_i, i = 1, ..., n\}$.

Following time-based analysis, frequency analysis of each S2 segment was performed extracting spectral roll-off (85%), centroid, and peak frequency [7]. Short-time spectral analysis was performed on the S2, subdivided into smaller windows, and the spectrum estimated (Hamming window). The spectral features previously referred were then extracted from the maximum energy window.

Finally, the order 6 Daubechies wavelet transform was obtained, and energy distribution over the approximation and details at different levels (level 4) was extracted and incorporated in the features matrix [10].

D. Blood Pressure and Second Heart Sound Analysis

The features described in the previous section were divided into time, frequency, and wavelet based features. Features were extracted from each heart sound, for each patient, and median values of all detected S2s were assigned to each patient. Following, the median S2 features set for each patient, were used in a multivariate linear regression model of the MBP (Equation 4), and adjusted for the total data using the different features' sets (least square error minimization).

$$\widehat{MBP}_i = a_0 + a_1 x_1(i) + ... + a_l x_l(i) + e(i) \qquad (4)$$

where a_i is the estimated weight of attribute x_i on the estimation $\widehat{MBP}_i$.

For each features' set a stepwise feature selection was performed, and a linear multivariate model adjusted and evaluated using a leave-one-out approach (reduced number of data points available). Results are presented for the global model using total data, and for the leave-one-out evaluation.

E. Evaluation Criteria

According to the British Hypertension Society, requirements for Grade A BP monitors are that measurements within a 5 mmHg range includes at least 60% of data, measurements within 10 mmHg comply 85% of data, and measurements within 15 mmHg range include 95% of the data [12], [13]. Cumulative percentages were calculated for each.

Mean absolute error (MAE, Equation 5), mean absolute percentage error (MAPE, Equation 6), mean error (ME, Equation 7), and error standard-deviation were calculated. According to the US Association for the Advancement of Medical Instrumentation standard, a BP device must display MAE inferior to 5 mmHg, and an error standard-deviation inferior to 8 mmHg [1].

$$MAE = \frac{1}{m}\sum_{i=1}^{m}\left|MBP_i - \widehat{MBP}_i\right| \qquad (5)$$

$$MAPE(\%) = \frac{1}{m}\sum_{i=1}^{m}\frac{\left|MBP_i - \widehat{MBP}_i\right|}{MBP_i} \qquad (6)$$

$$ME = \frac{1}{m}\sum_{i=1}^{m} MBP_i - \widehat{MBP}_i \qquad (7)$$

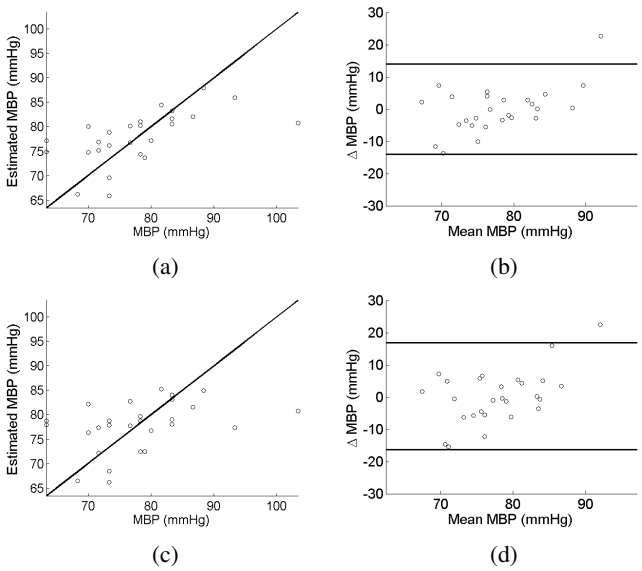

Fig. 5: Estimated Mean Blood Pressure (MBP): (a,c) measured MBP versus estimated; (b,d) Bland-Altman plot. (a,b) results for the linear model using all frequency features, and total data; (c,d) results for the leave-one-out adjusted model of frequency features.

where m is the number of patients.

For each set, the linear correlation coefficient was obtained, and to assess agreement between the BP measured by the conventional method, and the estimated, a Bland-Altman analysis was performed [14]. The mean of conventional method and estimated MBPs, and respective error and two standard-deviation boundaries are shown.

III. RESULTS AND DISCUSSION

Table II presents the results obtained for each model regarding correlation, and estimation errors, and Figure 5 presents the Bland-Altman plots for the error analysis of the frequency features set model, which exhibited lower error.

The best results in the cross-validation were obtained for the model using the S2 spectral features, which relation has also been reported in the literature [7], [4], followed by the wavelet subset, and time-based features. Figure 5, presenting the Bland-Altman analysis, shows that estimations have a wide variation, with no apparent relation between the mean MBP and the error. In [5] the authors propose a series of S2 features and several machine learning techniques, including a multivariate linear regression, to estimate the pulmonary arterial pressure. The best results obtained in this study were with support vector machines with radial basis function, and with a multilayer perceptron neural network (standard estimate of error of 5.6 and 8.3 mmHg, respectively). Their results were an improve to the previously published results, especially since the validation set was independent from the training set. Regarding systemic BP, in [4], the normalized spectrum of S2 was used to estimate SBP, and demonstrated a good correlation between the intra-arterial BP measurements and the estimated pressure via the acoustic method

TABLE II: Model results of estimated blood pressure, using S2 characteristics, in relation to measured blood pressure: correlation coefficient (ρ), mean absolute error (MAE), mean absolute percentage error (MAPE), mean error (ME), error standard-deviation (SD), and percentage estimates within error bands of 5, 10 and 15 mmHg.

						% Estimates Within Error Band		
Features	ρ	MAE (<5)	MAPE (%)	ME	Error SD (<8)	5 mmHg (>60%)	10 mmHg (>85%)	15 mmHg (>95%)
Total Data Linear Model								
Total	0.82	4.11	5.28	0.00	5.03	62.96	100.00	100.00
Time	0.40	5.91	7.48	0.00	8.05	48.15	85.19	92.59
Frequency	0.60	5.03	6.54	0.00	7.03	66.67	85.19	96.30
Wavelet	0.36	5.98	7.62	0.00	8.20	55.56	81.48	96.30
Leave-One-Out Adjusted Linear Model								
Total	0.22	7.48	9.69	-0.12	9.98	44.44	70.37	88.89
Time	-0.37	9.18	11.85	-0.88	12.66	37.04	70.37	77.78
Frequency	0.39	6.08	7.85	0.31	8.29	48.15	81.48	88.89
Wavelet	0.23	6.22	7.92	-0.22	8.81	48.15	81.48	92.59

proposed, reporting a mean relative error of 6%, nonetheless this methodology was for estimations following individual calibration.

The preliminary results presented in this study are similar to the results presented in the literature. Limitations in our study are the reduced number of patients, use of a children population (not homogenous), the fact that only one measure of BP was obtained for each patient not allowing for the individual calibration and repeatability analysis, and the limited range of BPs evaluated. Also, the linear multivariate model may not be adequate, since these features may exhibit non-linear relations to the BP [5]. A MAE of 6.08 mmHg was observed in the leave-one-out cross-validation of the frequency features set, which although is below the required standards for BP monitors, present as encouraging results for this exploratory study. We must highlight that the heart sound characteristics may be linked to normal physiological changes during growth, that should be analyzed in detail.

IV. CONCLUSIONS

The relation between systemic BP and the characteristics of the S2 were analyzed. Noninvasive estimation of BP through heart sound analysis, would allow for a more safe noninvasive monitoring of BP in high risk patients, without the discomfort of a pressure cuff, or an invasive arterial catheter, ideal for a long-term monitoring [4], [5], [6].

Children PCGs were segmented into S1 and S2 components, and individual S2s analyzed, demonstrating that S2 characteristics are related to the measured MBP. The spectral features extracted from the S2s presented the best results, comparable to those presented in the literature; data from different patients was used, and the population in study is not homogeneous (age and physiological modifications); probably it will be necessary to provide individual calibration for more reliable measurements within the same patient, in accordance with the current clinical practice [4].

This is an exploratory study, with some limitations, namely the small range of BP variations and an unique BP measurement for each patient. Other factors may induce bias such as S2 detection errors. In future studies, heart sounds and invasive systemic BP wave will be analyzed in conjunction, during abrupt changes of the BP in real clinical situations, to better understand the individual dynamic relations between BP, heart sounds, and patients' biotype.

REFERENCES

[1] J. Sola, M. Proenca, D. Ferrario, J.-A. Porchet, A. Falhi, O. Grossenbacher, Y. Allemann, S. Rimoldi, and C. Sartori, "Noninvasive and nonocclusive blood pressure estimation via a chest sensor," *Biomedical Engineering, IEEE Transactions on*, vol. 60, no. 12, pp. 3505–3513, 2013.

[2] *Global atlas on cardiovascular disease prevention and control*. World Health Organization, 2011.

[3] V. Chandrasekaran, R. Dantu, S. Jonnada, S. Thiyagaraja, and K. Subbu, "Cuffless differential blood pressure estimation using smart phones," *Biomedical Engineering, IEEE Transactions on*, vol. 60, no. 4, pp. 1080–1089, 2013.

[4] A. Bartels and D. Harder, "Non-invasive determination of systolic blood pressure by heart sound pattern analysis," *Clinical Physics and Physiological Measurement*, vol. 13, no. 3, pp. 249 –256, 1992.

[5] R. Smith and D. Ventura, "A general model for continuous noninvasive pulmonary artery pressure estimation," *Computers in Biology and Medicine*, vol. 43, no. 7, pp. 904 – 913, 2013.

[6] J. Xu, L.-G. Durand, and P. Pibarot, "Extraction of the aortic and pulmonary components of the second heart sound using a nonlinear transient chirp signal model," *Biomedical Engineering, IEEE Transactions on*, vol. 48, no. 3, pp. 277 –283, 2001.

[7] P. Arnott, G. Pfeiffer, and M. Tavel, "Spectral analysis of heart sounds: Relationships between some physical characteristics and frequency spectra of first and second heart sounds in normals and hypertensives," *Journal of Biomedical Engineering*, vol. 6, no. 2, pp. 121 – 128, 1984.

[8] A. Guyton and J. E. Hall, eds., *Textbook of Medical Physiology*. Elsevier Saunders, 11th ed., 2006.

[9] *Vander's Human Physiology: The Mechanisms of Body Function*. McGraw-Hill, 2001.

[10] A. Castro, T. T. V. Vinhoza, S. S. Mattos, and M. T. Coimbra, "Heart sound segmentation of pediatric auscultations using wavelet analysis," in *Engineering in Medicine and Biology Society, 2013 Proceedings of the 35th Annual International Conference of the IEEE*, 2013.

[11] A. Yadollahi and Z. Moussavi, "A robust method for heart sounds localization using lung sounds entropy," *Biomedical Engineering, IEEE Transactions on*, vol. 53, pp. 497–502, March 2006.

[12] E. O'Brien, T. Pickering, R. Asmar, M. Myers, G. Parati, J. Staessen, T. Mengden, Y. Imai, B. Waeber, and P. Palatini, "Working group on blood pressure monitoring of the european society of hypertension international protocol for validation of blood pressure measuring devices in adults," *Blood Pressure Monitoring*, vol. 7, no. 1, pp. 3–17, 2002.

[13] E. O'Brien, N. Atkins, G. Stergiou, N. Karpettas, G. Parati, R. Asmar, Y. Imai, J. Wang, T. Mengden, and A. Shennan, "European society of hypertension international protocol revision 2010 for the validation of blood pressure measuring devices in adults," *Blood Pressure Monitoring*, vol. 15, no. 1, pp. 23–38, 2010.

[14] J. M. Bland and D. G. Altman, "Statistical methods for assessing agreement between two methods of clinical measurement," *Lancet*, vol. 1, pp. 307–310, 1986.